

Influence of ground conductivity models on GIC hazard estimation in Germany

Leonie Pick¹, Alexander Grayver², Aline Guimarães Carvalho¹, Jens Berdermann¹

¹ German Aerospace Center (DLR), Institute for Solar-Terrestrial Physics; ² University of Cologne, Institute for Geophysics and Meteorology

1 Introduction

The hazard posed by **Geomagnetically Induced Currents (GICs)** to the regular operation of grounded infrastructure originates from the **induced geoelectric field (GEF)** under geomagnetically disturbed conditions. Here, we calculate GEF maps for Germany during 5 geomagnetic storms using **three different conductivity models** and evaluate their local agreement with independent

electric field records, their differences across the country, and their role in driving GICs at selected substations. Section 2 provides the storm characteristics and illustrates the production of geomagnetic disturbance maps, which are ensured to reproduce the independent magnetic field records from the permanent **magnetotelluric (MT) reference station** in Wittstock. Section 3 introduces the conductivity models and outlines their

usage in the adopted GEF calculation scheme.

Section 4 shows the comparison of modeled and measured GEFs at Wittstock while section 5 explores the differences in modeled GEFs across Germany.

Section 6 adds calculated GIC time series driven by the modeled GEFs at a selected substation in the northwestern section of the German high-voltage transmission grid.

2 Geomagnetic field

We obtain 1-min horizontal geomagnetic field observations from ≤ 11 INTERMAGNET stations in and around Germany (bdv, bel, bfe, bfo, clf, dou, fur, mab, ngk, wic, wng) for five 3-day geomagnetic storm intervals (Tab. 1) and apply the following processing steps:

1. **Baseline removal** [1] to isolate fast (<4h) variations (Fig. 1)
2. **SECS fit** [2] to produce disturbance map (Fig. 2)

#	Center date (12pm)	Max Kp	# Obs.	DE Rank [‡]	Max B _x [nT]	Max B _y [nT]	Max dB _x /dt [nT/min]	Max dB _y /dt [nT/min]
1	2012-03-15	6+	9	56	109	127	31.7	21.0
2	2013-10-02	8-	7 [◊]	37	124	148	34.7	42.5
3	2015-03-17	8-	8	14	328	342*	40.9	95.6
4	2017-09-08	8+	10	33	203	259	61.7	75.2
5	2021-05-12	7	9	62	122	104*	38.3	19.5

Tab. 1: Geom storm overview
Characteristics of selected geomagnetic storms based on INTERMAGNET observatory data.

[‡] Rank in sorted list of max. |dB/dt| averaged over ≥ 3 German obs. for each day since 2000
[◊] No data at BFO
* At NGK (all other at WNG)

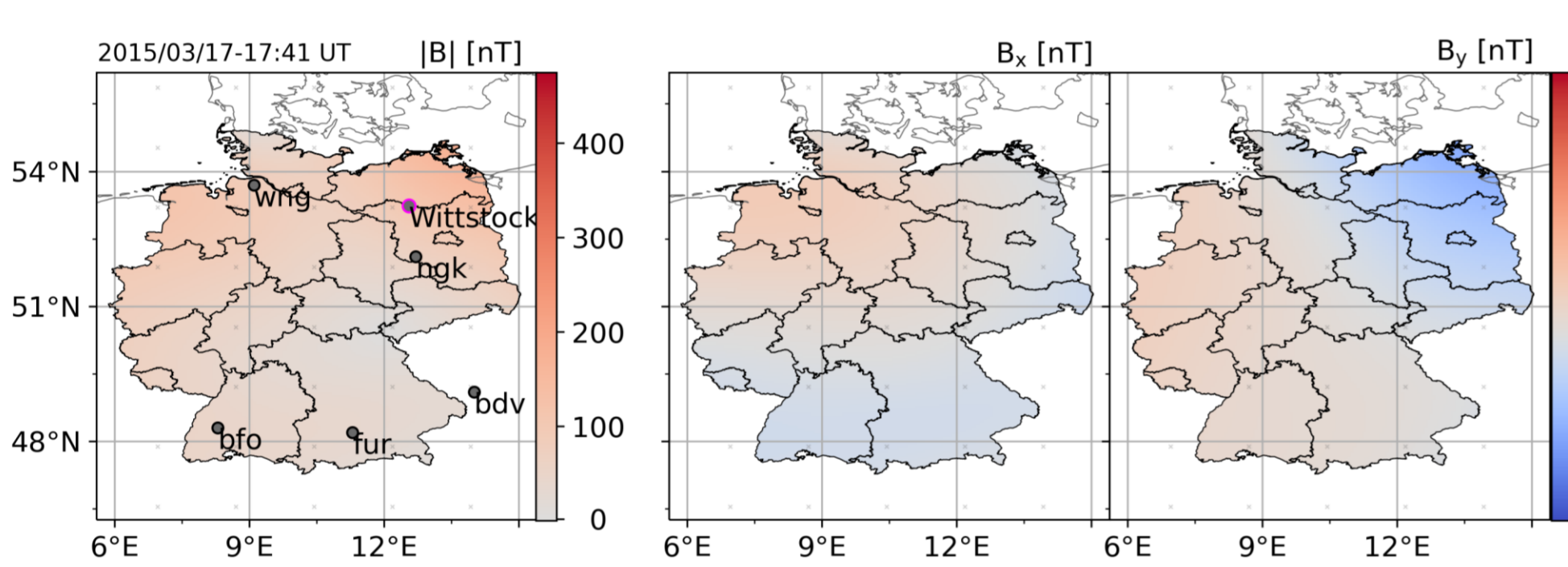


Fig. 1 (above): St. Patrick's Day storm at Wittstock
Northward (X, top) and eastward (Y, bottom) geomagnetic disturbance from Wittstock MT station (black, see location in Fig. 1 [3]) compared to modeled disturbance (magenta) based on INTERMAGNET records from 8 different locations (colored, lowercase).

Fig. 2 (left): SECS-based disturbance map
Snapshot of modeled absolute (left) and vector magnetic disturbance (right) at time of max. |dB/dt| during St. Patrick's Day storm (see Fig. 1 gray vertical line).

3 Conductivity models

The induced electric field is calculated in frequency space (0.1-8.3mHz) under the **plane-wave assumption**,

$$\vec{E}(\omega) = \frac{Z(\omega)}{i\omega} \vec{B}(\omega) \text{ [V/m]},$$

where \vec{B} is taken to be the magnetic disturbance field (see Fig. 2) and Z is the **impedance tensor** $[\Omega]$, calculated from three different conductivity models (Tab. 2, Fig. 3).

#	Name	Horizontal resolution	Dim	Max. depth [km]	Components	Impedance calculation
1	EuRhoM [5]	irregular 100s km	1	≤ 202	Divers	1D [4]
2	Global Conductivity [6]	$1^\circ \times 1^\circ$	3	100	Ocean, sediments, crust, top of mantle	1D [4]
3	EuSigma (A. Grayver, under develop.)	irregular $\sim 0.025^\circ$	3(+1)	≤ 15 (~ 1800)	Ocean + sediments [7], land sediments [8], crust (100 Ω m), mantle (1D)	3D Cartesian induction solver [9]

Tab. 2: Conductivity models
Overview of conductivity model specifications and impedance extraction methods.

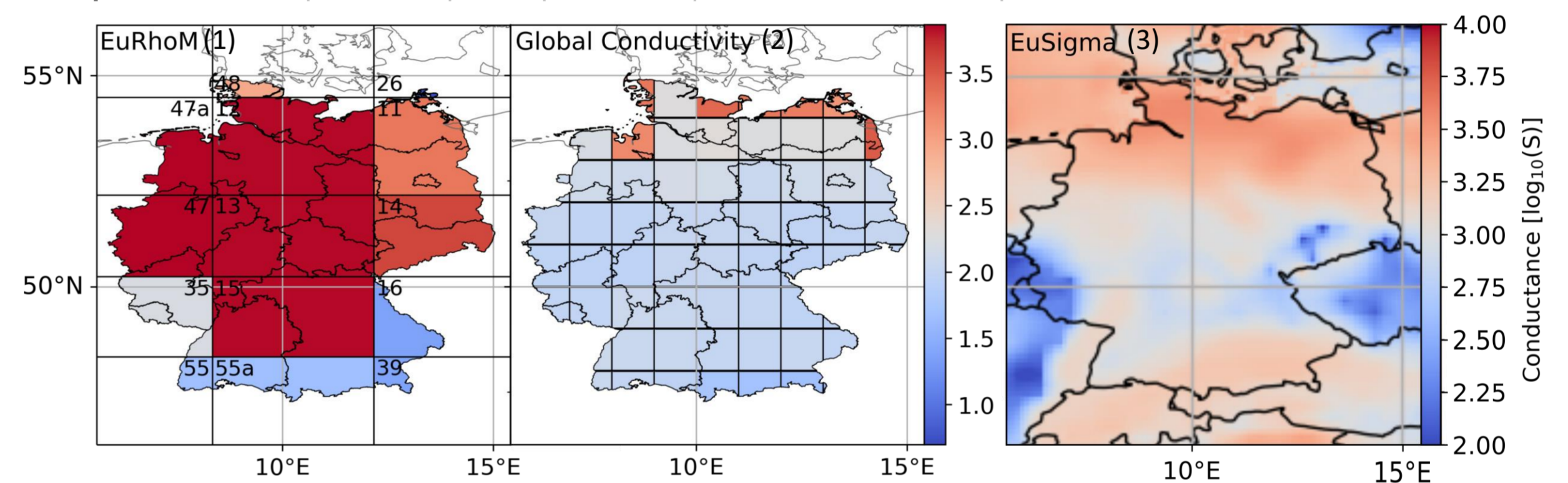


Fig. 3: Surface conductance maps

Surface conductance (depth-integrated conductivity) from three different conductivity models covering Germany (see Tab. 2).

4 Electric field at Wittstock

#	MAE _x [mV/km]			MAE _y [mV/km]		
	1	2	3	1	2	3
1	0.8	2.5	0.4	0.5	1.8	0.3
2	0.7	1.9	0.4	0.4	1.5	0.3
3	2.0	5.9	1.0	1.1	3.7	0.8
4	1.4	3.9	0.7	1.0	3.3	0.7
5	0.5	1.2	0.3	0.7	1.7	0.6

Tab. 3: GEF model errors
Mean absolute Error (MAE) between modeled GEFs and electric field observations from Wittstock MT station [3] in north (X) and east (Y) directions for all conductivity models (numbered columns, see legend of Fig. 4) and storms (rows).

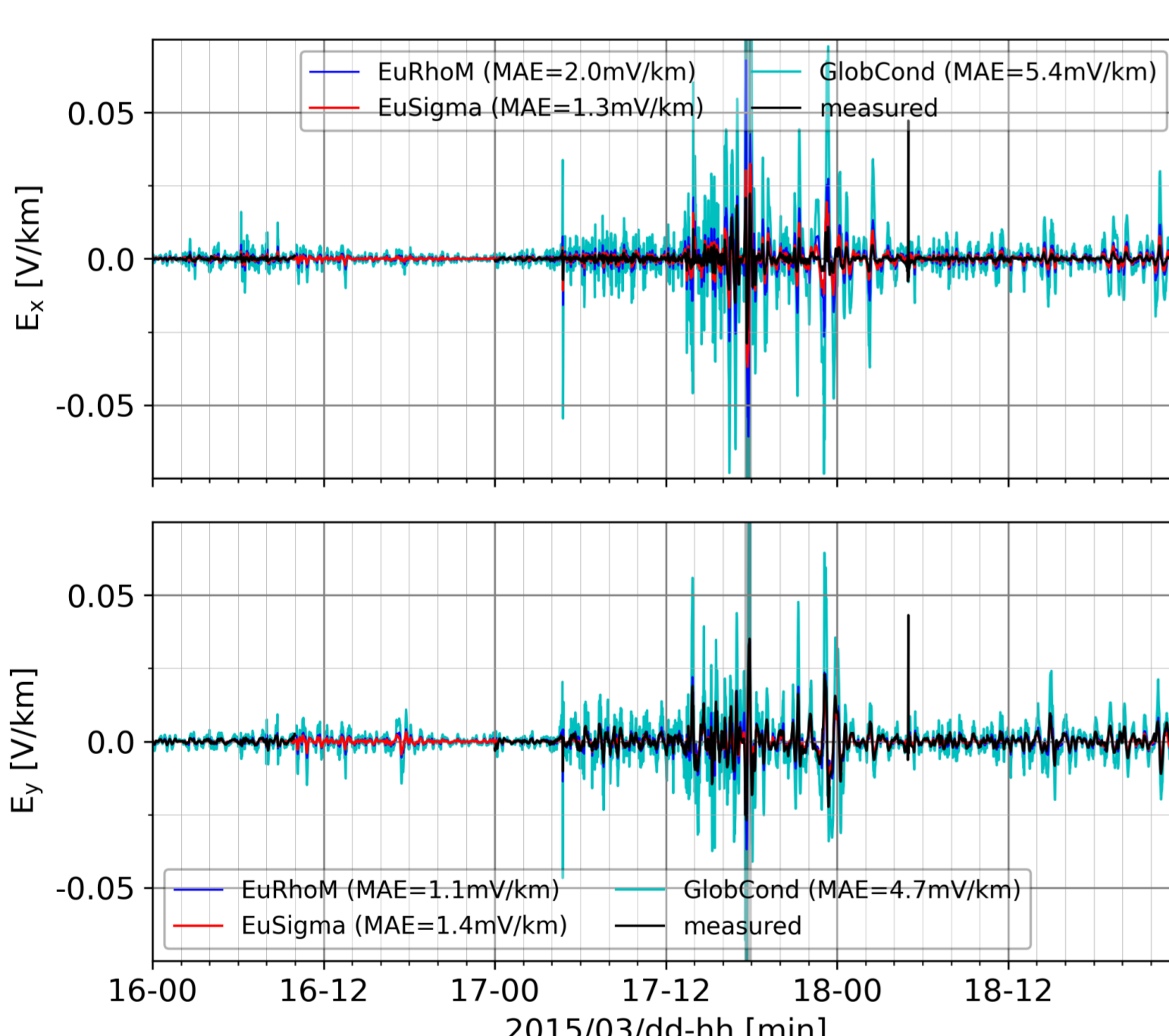


Fig. 4: St. Patrick's Day storm electric field at Wittstock
Measured (black) and modeled GEFs in north (top) and east (bottom) directions at Wittstock (location in Fig. 1) for three conductivity models (colored, see Tab. 2).

5 Electric field across Germany

#	Max E _x [V/km]			Max E _y [V/km]			Max ΔE _x [V/km]			Max ΔE _y [V/km]		
	1	2	3	1	2	3	1	2	3	1	2	3
#3	.310	.195	.131	.131	.134	.103	.245	.155	.227	.099	.101	.116
#5	.064	.038	.040	.100	.084	.080	.055	.028	.048	.082	.063	.071
Mean [1]	.194	.151	.372	.221	.177	.430	.183	.328	.354	.192	.391	.395
Std [1]	.065	.039	.069	.091	.032	.132	.061	.055	.086	.092	.092	.118

Tab. 4: Extreme & mean GEFs. Extreme GEFs (left) and GEF differences (right) for all conductivity models (see legend of Fig. 4) and 2 out of the 5 storms (top rows). Spatial means and standard deviations of storm-time averaged (5 snapshots per component), [0,1]-normalized GEFs and GEF differences (bottom rows).

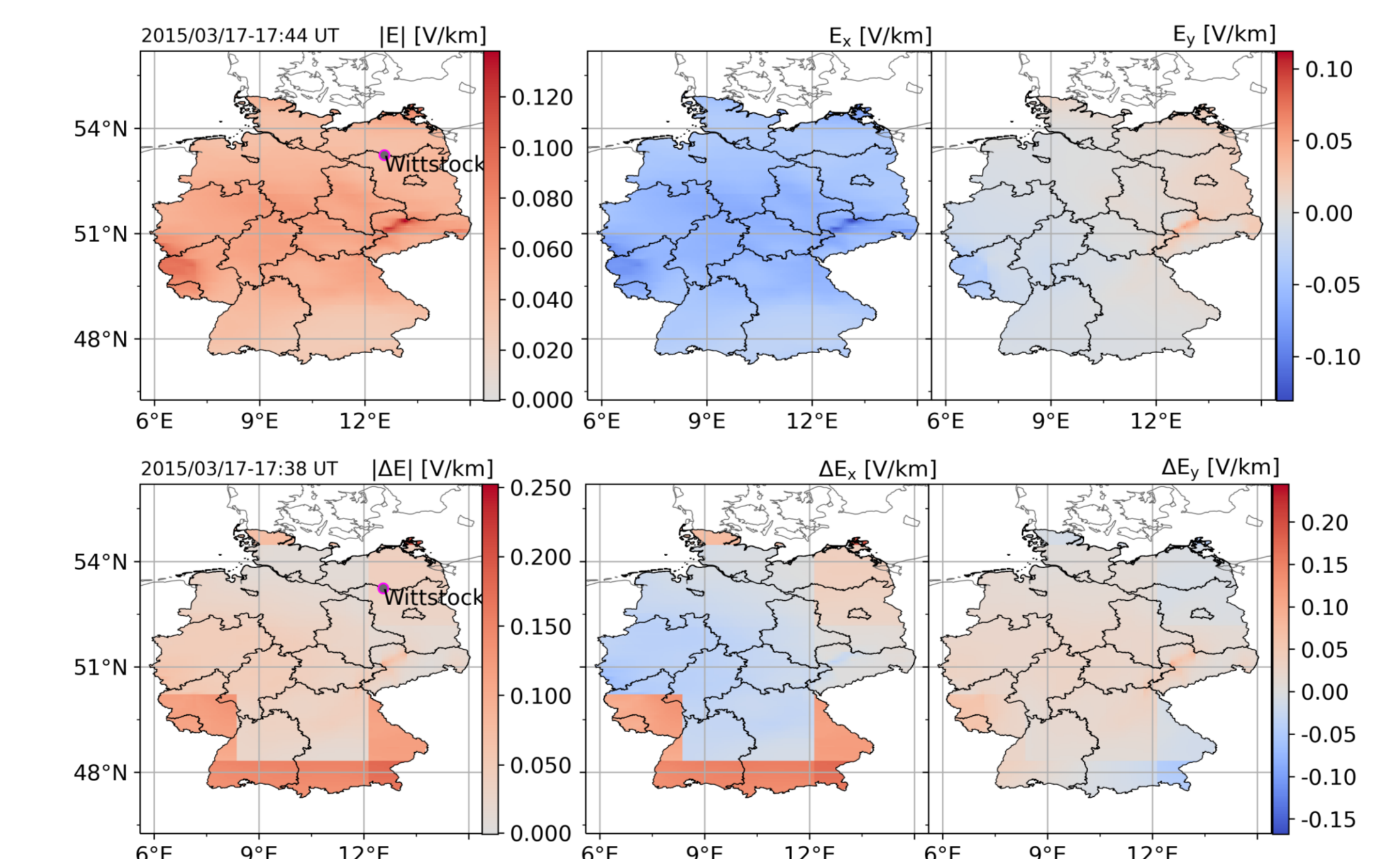


Fig. 5: St. Patrick's Day storm GEF maps. Snapshots of modeled absolute (left) and vector (right) GEF (for EuSigma, top) and GEF differences (between EuRhoM and EuSigma (Δ13), bottom) at times when extreme values are reached.

6 GIC at substation

The GEF drives a quasi-DC current through power lines and connected grounded transformers, which we calculate based on an ohmic model of the high-voltage grid (Fig. 6 & 7).

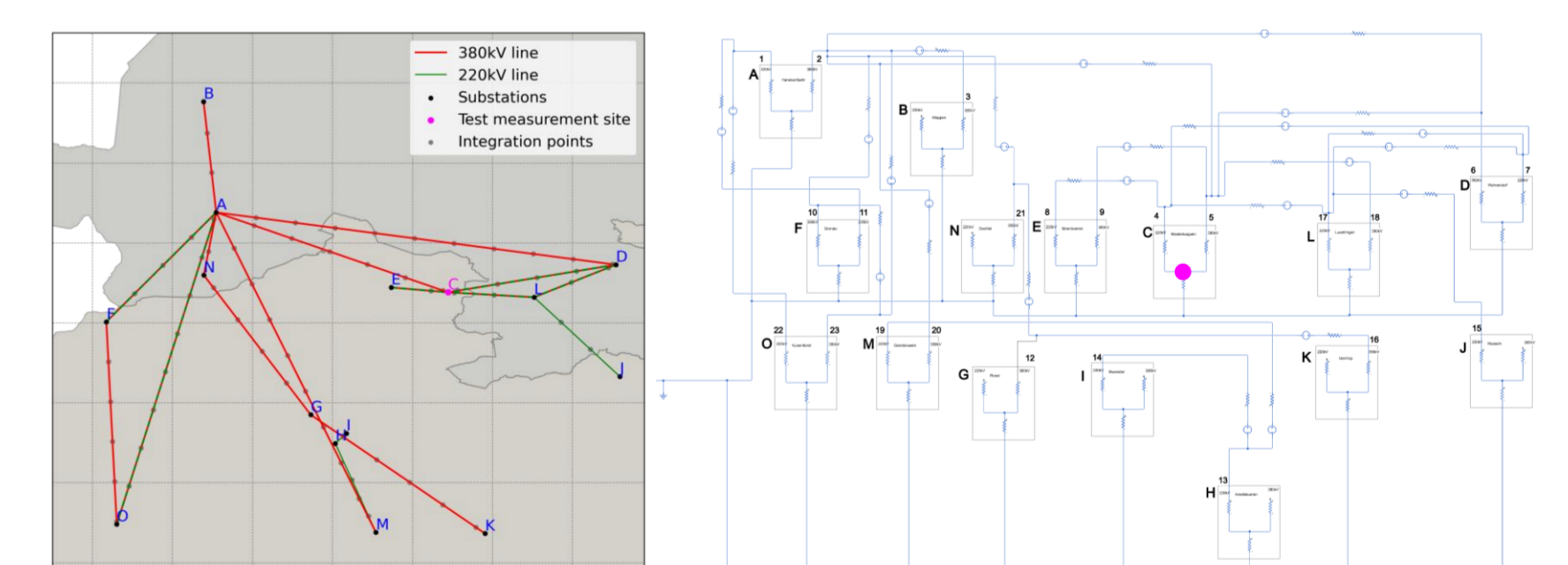


Fig. 6: High-voltage grid section
High-voltage lines and substations (labeled dots) in northwestern Germany (left) and corresponding circuit diagram including all direct connections to substation C (magenta).

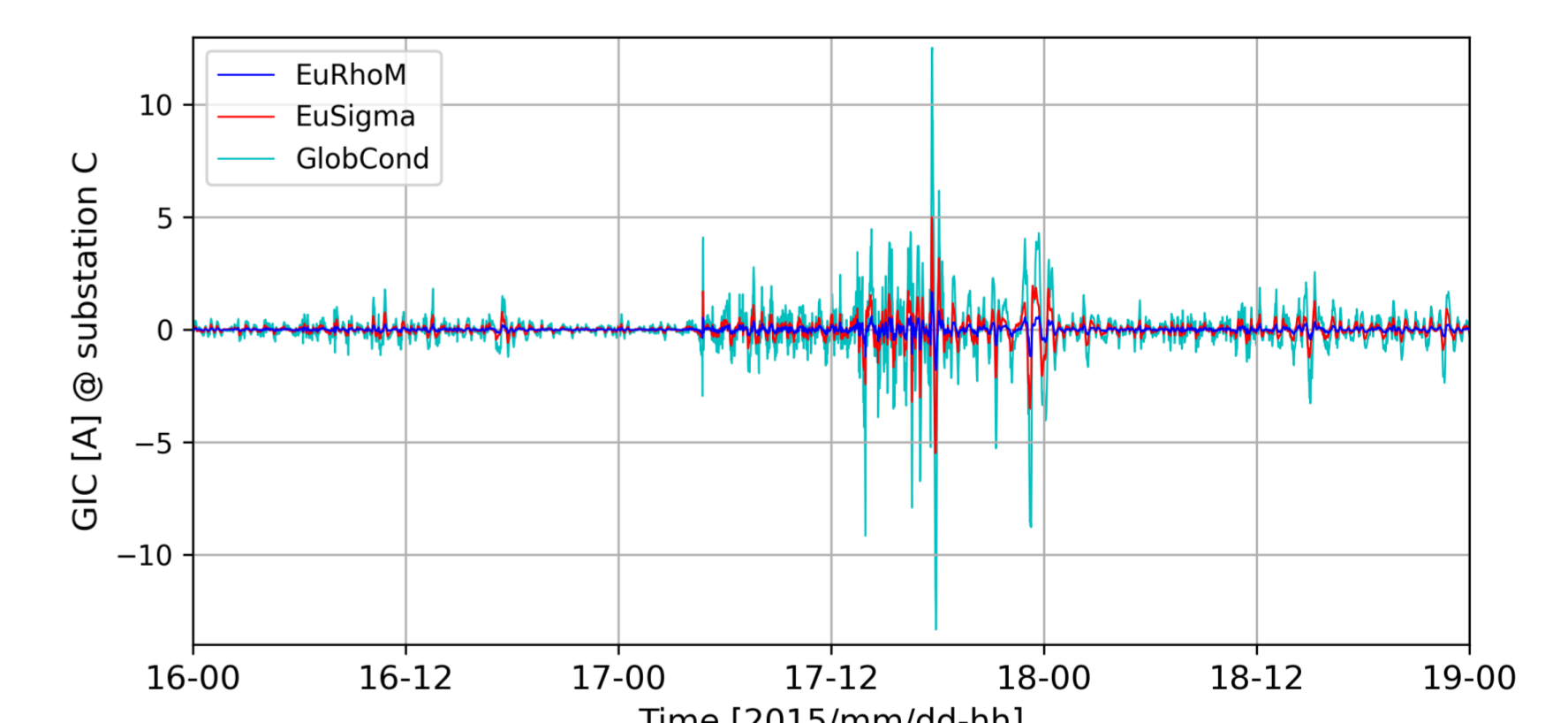


Fig. 7: St. Patrick's Day Storm GIC at substation in northwestern Germany
GEF-driven transformer neutral point current at substation C in northwestern Germany considering all direct connections in the high-voltage transmission grid (see Fig. 6).

7 Conclusions

- EuSigma-based GEF agrees best with measured electric field at Wittstock in northeastern Germany (MAE_x ≤ 1 mV/km, MAE_y ≤ 0.8 mV/km).
- EuSigma-based GEF shows smallest local extremes ($|E_{x,y}|_{\max} = 0.13$ V/km), but largest storm-time means across Germany with relative standard deviations $\sigma_x \approx 19\%$, $\sigma_y \approx 31\%$.
- GEF difference amplitudes are comparable to GEF amplitudes and smallest between EuSigma and EuRhoM on average.
- GICs at northwestern substations reflect GEF amplitude ranking at Wittstock (GIC_{max} $\approx 5A$ EuSigma).

8 Outlook

- Incorporate 1s-data from German geomagnetic observatories for selected events
- Explain uncertainties in modeled GEF: inaccuracies in impedance vs. magnetic field representation
- Update EuSigma
- Generate GIC threat map based on historic GEF
- Extend the grid model and update its parameters (esp. winding and grounding resistances)
- Verify complete GIC modeling chain by comparing results to measured GICs for 2023 storms

References

- [1] van de Kamp, M. (2013), Harmonic quiet-day curves as magnetometer baselines for ionospheric current analyses, *Geosci. Instrum. Method Data Syst.*, 2, 289-304
- [2] Amm, O. and Viljanen, A. (1999), Ionospheric disturbance magnetic field continuation from the ground to the ionosphere using spherical elementary current systems, *Earth, Planets and Space*, 51, 431-440
- [3] Ritter, O. et al. (2015), Permanent Magnetotelluric Reference Station in Wittstock, Germany (Datasets), *GFZ Data Services*, DOI: <http://doi.org/10.2312/GFZ.b103-15092>
- [4] Boteler, D. H. (1994), Geomagnetically Induced Currents: Present Knowledge and Future Research, *IEEE Transactions on Power Delivery*, 9(1)
- [5] Adám, A. et al. (2012), Estimation of the electric resistivity distribution (EURHOM) in the European lithosphere in the frame of the EURISGIC WP2 Project, *Acta Geodaetica et Geophysica Hungarica*, 47(4), 377-387
- [6] Alekseev, D. et al. (2015), Compilation of 3D global conductivity model of the Earth for space weather applications, *Earth Planet Sp.*, 67, 108, <https://globalconductivity.ocean.ru/>
- [7] Grayver, A. V. (2021), Global 3-D electrical conductivity model of the world ocean and marine sediments. *Geochemistry, Geophysics, Geosystems*, 22, e2021GC009950
- [8] Tesaura, M. et al. (2008), EuCRUST-07: A new reference model for the European crust, *Geophys. Res. Lett.*, 35, L05313
- [9] Grayver, A. V. & Kolev, T. V. (2015), Large-scale 3D geoelectromagnetic modeling using parallel adaptive high-order finite element method, *GEOPHYSICS*, 80, E277-E291

Acknowledgments

We thank the operators of the INTERMAGNET geomagnetic observatories, Oliver Ritter and his colleagues from GFZ Potsdam for providing the Wittstock MT-Data, the providers of EuRhoM and Global Conductivity models, and a German TSO for cooperation.